Climate of the Past

Open Access

Supplement of

Nutrient utilisation and weathering inputs in the Peruvian upwelling region since the Little Ice Age

C. Ehlert et al.

Correspondence to: C. Ehlert (cehlert@mpi-bremen.de)

1 Age model for core M771-470

Core M771-470 was taken at 11° S, 77°56.6' W in 145 m water depth during cruise M77/1 with the German R/V Meteor in 2008 (Fig. 1). The age model was obtained by measuring excess ^{210}Pb activities and modeling the resulting profiles as described by Meysman et al. (2005) (Fig. S1, Table S1). Porosity data for core M771-470 were determined from water loss after freeze-drying. The fit to the porosity data was obtained by applying Φ_0 (porosity at the sediment water interface) = 0.95, Φ_f (porosity at infinite depth after steady state compaction) = 0.85, p (attenuation constant) = 0.02 cm^{-1}. Excess ^{210}Pb was modelled based on a fit to the data obtained with $D_B(0)$ (bioturbation coefficient at the sediment water interface) = 30 cm^2 yr^{-1}, xs (sediment depth where $D_B(x)$ is approaching a value of zero) = 7 cm, A_I (^{210}Pb activity of the particles raining to the seafloor) = 3.4 Bq g^{-1}, w_f (burial velocity) = 48 cm kyr^{-1}. These results indicate bioturbation in the uppermost 10 cm. The average sedimentation rate of core M771-470 between 10 and 25cm profile depth of 0.92 mm/yr is essentially identical to the one obtained from the nearby core SO147-106KL for the time period 1400-1900 AD of 0.9 mm/yr (Rein et al., 2004).

The porosity data show a pronounced decrease between 24 cm and 32 cm profile depth (Fig. S.1a and Fig. 2, Table S.1), which is considered to reflect a sedimentological feature that marks the transition of the LIA towards modern conditions (= transition period). This shift can be found in several cores from the region and has been dated to start ~1820 AD, with an uncertainty of 10-15 years (Gutiérrez et al., 2009; Salvatteci et al., in review). The highest values of bSi that can be found in ~25 cm profile depth in core M771-470 are recorded in several cores off Peru and Chile just after the LIA during the transition period (Gutiérrez et al., 2009; Díaz-Ochoa et al., 2011; Salvatteci et al. in review), suggesting a regional event. Using average sedimentation rates from the nearby core B0405-13 (12°S, 184 m water depth) of ~1.8 mm/yr for the modern sediments from the time period 1870-1952 AD, ~1.5 mm/yr for the transition period between 1818-1870 AD and lower sedimentation rates of 0.6 mm/yr during the LIA from ca. 1300-1818 AD (Gutiérrez et al., 2009) would indicate, that the core depth between 26 cm and 32 cm corresponds to the transition period, shallower depths reflect modern sediments and deeper depths reflect sediments from the LIA. This was adopted for the discussion in the manuscript.

2 Leachate neodymium isotope composition

2.1 Methods

To obtain the radiogenic isotope composition of past bottom seawater at the sites of the sediment cores from the early diagenetic Fe-Mn coatings of the sediment particles, previously published methods were applied (Gutjahr et al., 2007; Stumpf et al., 2010). First, the carbonate fraction was removed from the freeze-dried and homogenized sediment samples using a 15%-acetic acid/1 M Na-acetate buffer solution. Afterwards, the authigenic Fe-Mn oxyhydroxide fraction was leached and separated from the sediment with a 0.05 M hydroxylamine hydrochloride/15%-acetic acid solution buffered with NaOH to pH 3.8. For purification of the leachate fraction and analyses of Nd and Sr isotope composition please refer to the main text.

2.2 Changes in Subsurface Water Masses

The $\varepsilon_{Nd\ coating}$ record of core M771-470 only shows a small variability ranging from -1.2 to -2.3 with a mean value of -1.7 ± 0.7 ($2\sigma_{(sd)}$) and no significant trends are observable (Fig. S2, Table S2). For core B0405-6 no $\varepsilon_{Nd\ coating}$ signature could be determined because the available amount of left over sediment material was not sufficient.

Knowledge about changes in the origin of the subsurface waters would help to better constrain some of the changes in utilisation discussed, i.e. concerning the source regions (northern or southern) of the water masses and therefore which pre-formed (utilisation) signal should be assumed. Early diagenetic Fe-Mn coatings in marine sediments have been shown to archive the dissolved ε_{Nd} signature of (bottom) water masses, which had been acquired in the source regions of water masses via weathering of continental rocks with distinct isotopic signatures and supply to the ocean via rivers, eolian input or through shelf exchange processes (Frank, 2002; Lacan and Jeandel, 2005). The Eastern Equatorial Pacific is influenced by two main water mass sources. The Central Pacific is characterised by more radiogenic signatures around -2 and waters of this origin are supplied to the EEP via the EUC/PCUC (Fig. 1) (Lacan and Jeandel, 2001; Grasse et al., 2012). In contrast, the water masses of Southern Ocean origin are characterised by less radiogenic signatures

around -8 (Piepgras and Jacobsen, 1988; Grasse et al., 2012). Core M771-470 is located in 145 m water depth, which is in the present day core depth of the PCUC (Fig. 1) (Brink et al., 1983). The $\varepsilon_{Nd\,coating}$ signature in core M771-470 ranges between -1.2 and -2.3, which suggests that the signature has not deviated significantly from the composition of the present-day PCUC (Grasse et al., 2012; Ehlert et al., 2013). As described above, the PCUC is the predominant bottom current at the location of the core under strong upwelling conditions. When upwelling was weak the surface currents could expand both latitudinally and vertically within the water column and may also have impacted the bottom water signatures (Montes et al., 2011). However, as described by Ehlert et al. (2013), the variability of the $\varepsilon_{Nd\,coating}$ signature on the Peruvian shelf has not necessarily only been related to the prevalent current regime and water mass mixing but exchange between bottom waters and the underlying sediments and the pore waters plays an important role, in particular under oxygen-depleted conditions in the sediments and bottom waters (Haley et al., 2004; Lacan and Jeandel, 2005), which prevents a reliable assessment of past water mass mixing based on the Nd isotope composition of the coatings. This is the reason why the data for the one core are not included in the discussion of the main text and only provided here for completeness.

Supplementary references

Brink, K. H., Halpern, D., Huyer, A., and Smith, R. L.: The Physical Environment of the Peruvian Upwelling System, Progress in Oceanography, 12, 285–305, 1983.

Díaz-Ochoa, J. A., Pantoja, S., De Lange, G. J., Lange, C. B., Sánchez, G. E., Acuña, V. R., Muñoz, P., and Vargas, G.: Oxygenation variability in Mejillones Bay, off northern Chile, during the last two centuries, Biogeosciences, 8(1), 137–146, 2011. doi:10.5194/bg-8-137-2011

Ehlert, C., Grasse, P., and Frank, M.: Changes in silicate utilisation and upwelling intensity off Peru since the Last Glacial Maximum - insights from silicon and neodymium isotopes, Quaternary Science Reviews, 72, 18–35, 2013. doi:10.1016/j.quascirev.2013.04.013

1   Frank, M.: Radiogenic isotopes: tracers of past ocean circulation and erosional input,

2   Reviews of Geophysics, 40(1), 2002. doi:10.1029/2000RG000094

3   Grasse, P., Stichel, T., Stumpf, R., Stramma, L., and Frank, M.: The distribution of

4   neodymium isotopes and concentrations in the Eastern Equatorial Pacific: Water mass

5   advection versus particle exchange, Earth and Planetary Science Letters, 353-354,

6   198–207, 2012. doi:10.1016/j.epsl.2012.07.044

7   Gutiérrez, D., Sifeddine, A., Field, D. B., Ortlieb, L., Vargas, G., Chavez, F. P.,

8   Velazco, F., Ferreira-Bartrina, V., Tapia, P. M., Salvatteci, R., Boucher, H., Morales,

9   M. C., Valdés, J., Reyss, J.-L., Campusano, A., Boussafir, M., Mandeng-Yogo, M.,

10   García, M., and Baumgartner, T.: Rapid reorganization in ocean biogeochemistry off

11   Peru towards the end of the Little Ice Age, Biogeosciences, 6, 835–848, 2009.

12   Gutjahr, M., Frank, M., Stirling, C. H., Klemm, V., Van de Flierdt, T., and Halliday,

13   A. N.: Reliable extraction of a deepwater trace metal isotope signal from Fe–Mn

14   oxyhydroxide coatings of marine sediments, Chemical Geology, 242, 351–370, 2007.

15   doi:10.1016/j.chemgeo.2007.03.021

16   Haley, B. A., Klinkhammer, G. P., and McManus, J.: Rare earth elements in pore

17   waters of marine sediments, Geochimica et Cosmochimica Acta, 68(6), 1265–1279,

18   2004. doi:10.1016/j.gca.2003.09.012

19   Lacan, F., and Jeandel, C.: Tracing Papua New Guinea imprint on the central

20   Equatorial Pacific Ocean using neodymium isotopic compositions and Rare Earth

21   Element patterns, Earth and Planetary Science Letters, 186, 497–512, 2001.

22   Lacan, F., and Jeandel, C.: Neodymium isotopes as a new tool for quantifying

23   exchange fluxes at the continent − ocean interface, Earth and Planetary Science

24   Letters, 232, 245–257, 2005. doi:10.1016/j.epsl.2005.01.004

25   Meysman, F. J. R., Boudreau, B. P., and Middelburg, J. J.: Modeling reactive

26   transport in sediments subject to bioturbation and compaction, Geochimica et

27   Cosmochimica Acta, 69(14), 3601–3617, 2005. doi:10.1016/j.gca.2005.01.004

1 Montes, I., Schneider, W., Colas, F., Blanke, B., and Echevin, V.: Subsurface
2 connections in the eastern tropical Pacific during La Niña 1999 – 2001 and El Niño
3 2002 – 2003, Journal of Geophysical Research, 116(C12022), 2011.
4 doi:10.1029/2011JC007624

5 Piepgras, D. J., and Wasserburg, G. J.: Isotopic Composition of Neodymium in
6 Waters from the Drake Passage, Science, 217, 207–214, 1982.

7 Rein, B., Lückge, A., and Sirocko, F.: A major Holocene ENSO anomaly during the
8 Medieval period, Geophysical Research Letters, 31(L17211), 2004.
9 doi:10.1029/2004GL020161

10 Salvatteci, R., Field, D. B., Sifeddine, A., Ortlieb, L., Ferreira-Bartrina, V.,
11 Baumgartner, T., Caquineau, S., Velazco, F., Reyss, J.-L., Sanchez-Cabeza, J. A., and
12 Gutiérrez, D.: Cross-stratigraphies from a seismically active mud lens off Peru
13 indicate horizontal extensions of laminae, missing sequences, and a need for multiple
14 cores for high resolution records, Marine Geology (in review).

15 Stumpf, R., Frank, M., Schönfeld, J., and Haley, B. A.: Late Quaternary variability of
16 Mediterranean Outflow Water from radiogenic Nd and Pb isotopes, Quaternary
17 Science Reviews, 49, 1–11, 2010. doi:10.1016/j.quascirev.2010.06.021

18

1   Table S1. Core M771-470 a) excess ^{210}Pb measurements and porosity data, b) age
2   model based on sedimentation rates from Gutiérrez et al. (2009), and $^{143}Nd/^{144}Nd$, ε_{Nd}
3   and $^{87}Sr/^{86}Sr$ of authigenic Fe-Mn coatings. $2\sigma_{(sd)}$ represents the external
4   reproducibilities of repeated standard measurements.

a) 210Pb-dating and porosity				b) age model							
depth (cm)	^{210}Pb (Bq/kg)	error (Bq/kg)	porosity	depth (cm)	Sed. rate*	year AD	$^{143}Nd/^{144}Nd$	ε_{Nd}	$2\sigma_{(sd)}$	$^{87}Sr/^{86}Sr$	$2\sigma_{(sd)}$
0 - 1	-	-	0.953								
1 - 2	1.14E+03	7.34E+01	0.944	1.5		1976	0.512539	-1.9	0.3	0.709030	2.6E-05
2 - 3	-	-	0.945	3.5		1965	0.512551	-1.7	0.3	0.708971	2.6E-05
3 - 4	9.42E+02	5.97E+01	0.940	5.5		1954	0.512546	-1.8	0.3	0.709080	2.6E-05
4 - 5	-	-	0.932	9	1.8 mm/yr	1934	0.512556	-1.6	0.3	0.709099	2.6E-05
5 - 6	-	-	0.938	11		1923	0.512526	-2.2	0.3	0.709121	2.6E-05
6 - 8	9.84E+02	6.36E+01	0.955	15		1901	0.512521	-2.3	0.3	0.709112	2.6E-05
8 - 10	7.75E+02	5.35E+01	0.935	19		1879	0.512559	-1.5	0.3	0.709094	2.6E-05
10 - 12	5.28E+02	3.74E+01	0.928	20		1873	0.512571	-1.3	0.3	0.708748	8.0E-06
12 - 14	2.66E+02	2.57E+01	0.925	23		1853	0.512547	-1.8	0.3	0.709153	2.6E-05
16 - 18	8.68E+01	1.86E+01	0.920	25	1.5 mm/yr	1840	0.512539	-1.9	0.3	0.709132	2.6E-05
20 - 22	1.27E+02	1.97E+01	0.915	26		1833	-	-	-	0.708973	8.0E-06
22 - 24	9.49E+01	1.87E+01	0.920	27		1827	0.512542	-1.9	0.3	0.709130	2.6E-05
26 - 28	<2.28E+01	-	0.838	29		1803	0.512538	-2	0.3	0.709136	2.6E-05
28 - 30	<2.08E+01	-	-	32		1753	0.512523	-2.3	0.3	0.709140	2.6E-05
30 - 34	<1.89E+01	-	0.818	32 (dupl.)		1753	0.512564	-1.4	0.3	0.708935	5.0E-06
34 - 38	<2.22E+01	-	0.846	36	0.6 mm/yr	1687	0.512574	-1.2	0.3	0.708727	8.0E-06
40	-	-	0.822	40		1620	0.512565	-1.4	0.3	0.708928	8.0E-06
44	-	-	0.841	44		1553	0.512572	-1.3	0.3	0.708745	5.0E-06
48.5	-	-	0.839	48.5		1478	0.512564	-1.4	0.3	0.708847	5.0E-06

5   *average sedimentation rates were determined on nearby core B0405-13.

6
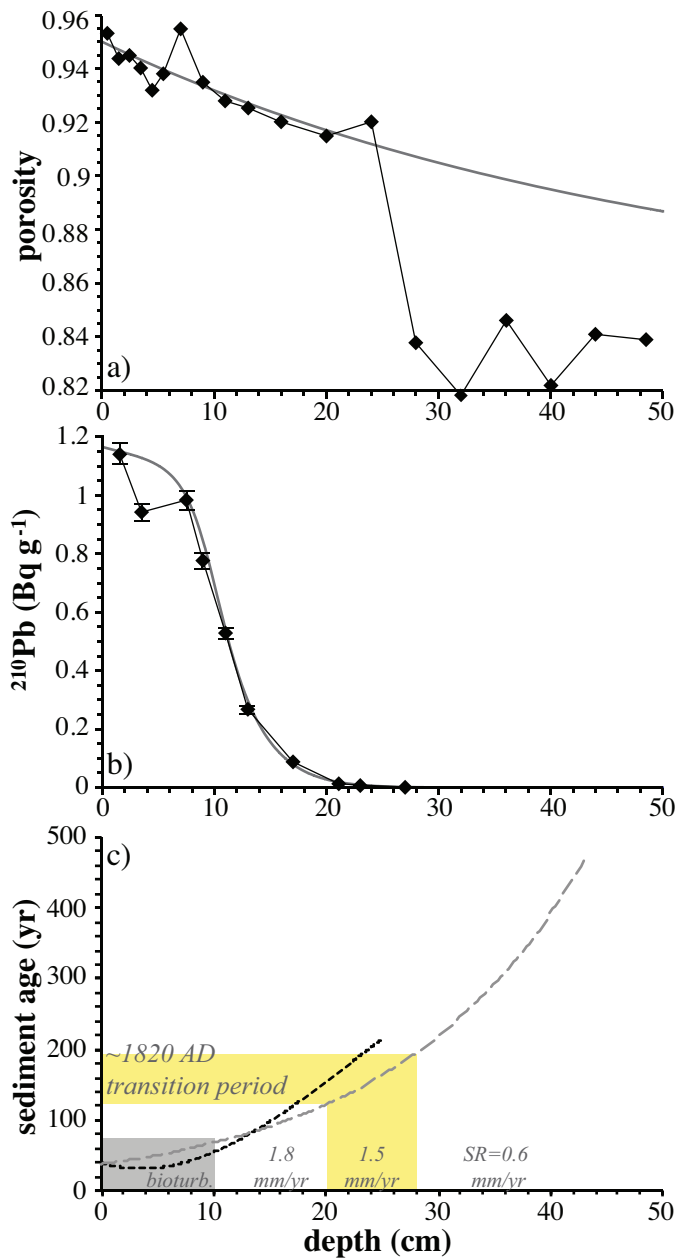
Figure S1. Age model for core M771-470 (data: black diamonds, best fit: grey line). a) porosity versus depth (cm), b) excess ^{210}Pb activity (Bq g[-1]), and c) resulting age/depth relationship (black curve = [210]Pb modeling, grey curve = using average sedimentation rates of core B0405-13 (Gutiérrez et al., 2009). The grey shading indicates the bioturbated zone, the yellow shading highlights the transition zone from the LIA to modern sediments.
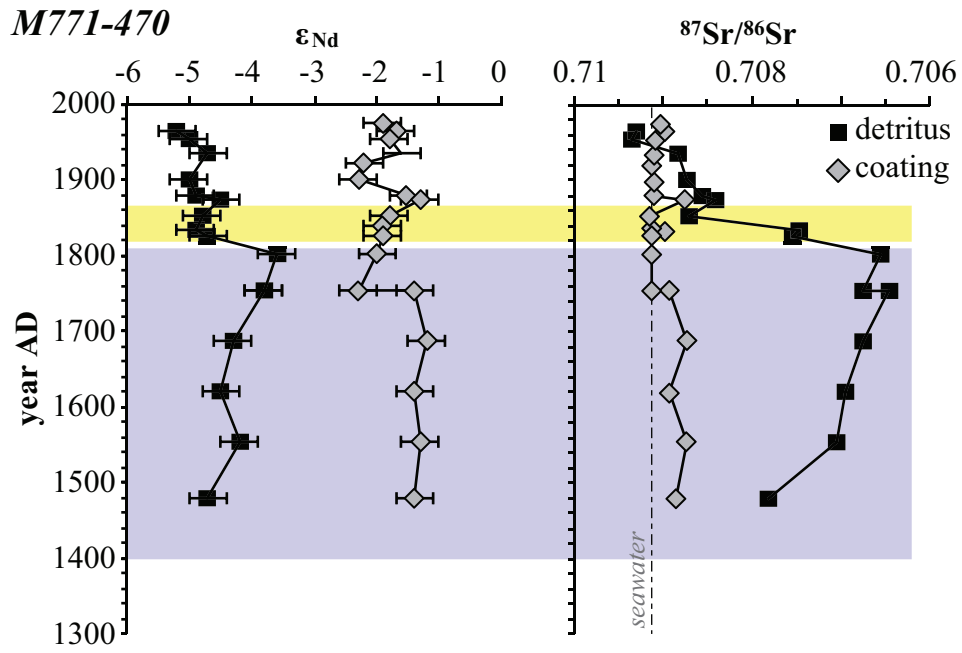
Figure S2. Downcore records for core M771-470 for ε_{Nd} and $^{87}Sr/^{86}Sr$ for authigenic Fe-Mn coatings (grey diamonds) and detrital material (black squares). Error bars represent $2\sigma_{(sd)}$ external reproducibilities of repeated standard measurements. The grey dashed line indicates the present day dissolved seawater $^{87}Sr/^{86}Sr$ of 0.70916. The blue shading indicates the LIA and the yellow shading represents the time span of the transition period.